Calibration on wide-ranging aluminum doping concentrations by photoluminescence in high-quality uncompensated p-type 4H-SiC

Satoshi Asada, Tsunenobu Kimoto and Ivan Gueorguiev Ivanov

Asada, S., Kimoto, T., Ivanov, I. G., (2017), Calibration on wide-ranging aluminum doping concentrations by photoluminescence in high-quality uncompensated p-type 4H-SiC, *Applied Physics Letters*, 111(7), . https://doi.org/10.1063/1.4989648

Original publication available at:
https://doi.org/10.1063/1.4989648

Calibration on wide-ranging aluminum doping concentrations by photoluminescence in high-quality uncompensated p-type 4H-SiC

Satoshi Asada,[1] Tsunenobu Kimoto,[1] and Ivan G. Ivanov[2]
[1)] *Department of Electronic Science and Engineering, Kyoto University, Katsura, Nishikyo, Kyoto 615-8510, Japan*
[2)] *Department of Physics, Chemistry and Biology, Linköping University, S-581 83, Linköping, Sweden*

(Dated: 7 October 2017)

Previous work has shown that the concentration of shallow dopants in a semiconductor can be estimated from the photoluminescence (PL) spectrum by comparing the intensity of the bound-to-the-dopant exciton emission to that of the free exciton. In this work we study the low-temperature PL of high-quality uncompensated Al-doped p-type 4H-SiC and propose algorithms for determining the Al-doping concentration using the ratio of the Al-bound to free-exciton emission. We use three different cryogenic temperatures (2, 41 and 79 K) in order to cover the Al-doping range from mid 10^{14} cm^{-3} up to 10^{18} cm^{-3}. The Al-bound exciton no-phonon lines and the strongest free-exciton replica are used as a measure of the bound- and free-exciton emissions at a given temperature, and clear linear relationships are obtained between their ratio and the Al-concentration at 2, 41, and 79 K. Since nitrogen is a common unintentional donor dopant in SiC, we discuss also the criteria allowing one to determine from the PL spectra whether a sample can be considered as uncompensated or not. Thus, the low-temperature PL provides a convenient non-destructive tool for evaluation of the Al concentration in 4H-SiC which probes the concentration locally and, therefore, can be used also for mapping the doping homogeneity.

4H-silicon carbide (4H-SiC) is a promising material for high-power and high-temperature device applications owing to its wide bandgap of 3.26 eV and high breakdown electric field of 2.8 MV/cm.[1–3] This semiconductor can be easily doped to n- and p-type (usually, with N and Al, respectively), but the precise control of doping concentrations in matured epitaxial growing techniques is of crucial importance for fabrication of high-performance devices. Thus, characterization methods which can accurately determine the doping concentration in the epilayers are desirable. There exist several common methods for this purpose, such as Hall-effect, capacitance-voltage (C–V), and secondary ion mass spectrometry (SIMS) measurements. These methods have revealed important electronic properties in both n- and p-type 4H-SiC.[4–11] However, these methods either require formation of contacts or destroy the specimens, which makes them inapplicable in wafer-scale characterization.

Photoluminescence (PL) is one convenient and non-destructive method for qualitative detection of many impurities and intrinsic defects in SiC.[12–14] Quantitative determination of the nitrogen doping concentration [N] using PL in uncompensated n-type 4H- and 6H-SiC has also been reported.[15–17] Quantitative determination of shallow impurities in silicon is known for a long time and is based on the fact that the ratio of the integrated PL intensity of the bound to the dopant excitons (BE) to that of free excitons (FE), $R = I_{\mathrm{BE}}/I_{\mathrm{FE}}$, is uniquely proportional to the doping concentration.[18] Thus, the doping concentration can be estimated from the PL spectrum by acquiring the intensity ratio. The method has been suggested first by M. Tajima to measure the boron and phosphorus concentrations in silicon[18] and analogous approaches have been adopted for several semiconductor materials such as Ge, GaAs, and n-type 4H- and 6H-SiC.[15–17,19–22] In addition, PL probes much smaller area of the sample than other conventional methods (determined by the size of the exciting-laser spot on the sample, typically $\sim$100 μm), which provides possibility for mapping the doping homogeneity.

Previous work[23] has investigated also the possibility for quantitative determination of the Al concentration (denoted [Al] hereafter) in unintentionally-doped compensated 4H-SiC using the ratio between the integrated emissions of the Al-bound (Al-BE) and N-bound (N-BE) excitons, but the resulting estimations are not very accurate and certainly unsuitable for uncompensated Al-doped p-type samples, because the N-bound exciton emission is hardly observable in such samples. Another work[24] proposes to use the broadening and/or the energy downshift of the Al-BE no-phonon lines as an indicator of the Al concentration, but both parameters exhibit measurable changes only for [Al] above mid-10^{18} cm^{-3}, thus limiting the possibility for [Al] estimation only to very high doping levels.

In this study, we use the ratio R of the integrated PL intensity of the Al-bound excitons to that of free excitons and acquire the linear relationship between R and [Al] at several temperatures (2, 41, 79 K). The measurements are performed on high-quality uncompensated p-type 4H-SiC epilayers covering the entire Al-concentration range from 5.8×10^{14} to 7.1×10^{18} cm^{-3}.

The samples are 100-μm-thick Al-doped p-type 4H-SiC epilayers grown on n-type 4H-SiC (0001) 4°-off-axis substrates. The net doping concentrations ($N_{\mathrm{A}} - N_{\mathrm{D}}$) as well as the individual Al-acceptor and N-donor concentrations in the epilayers have been carefully determined in previous work using C–V and Hall-effect measurements in

combination with SIMS.[10] The compensation ratio, i.e. N_D/N_A of all samples is below 1% except for the sample with the lowest doping concentration ([Al] = 5.8×10^{14} cm^{-3}), the ratio of which is about 7%. Free-standing epilayers from other pieces of the same samples were also prepared by polishing away the substrate down to thickness about 85 μm and finishing with chemical mechanical polishing. The free-standing films were also measured in PL in order to obtain additional information on the homogeneity of the doping, as well as on the contribution from the substrate in the PL spectra.

The PL spectra are taken at several cryogenic temperatures, which allows assessment of [Al] in different ranges of concentrations, as explained later. The setup consists of a single monochromator (Jobin Yvon, Model HR460) equipped with a 2400 grooves/mm grating and coupled to a CCD camera. The resulting resolution is about 0.6 Å (0.5 meV, with 50 μm slit). The samples are excited by the 351 nm ultraviolet line of an Ar ion laser, using < 5 mW power moderately focused on the sample to a spot diameter of approximately 100 μm, resulting in power density < 15 W/cm^2.

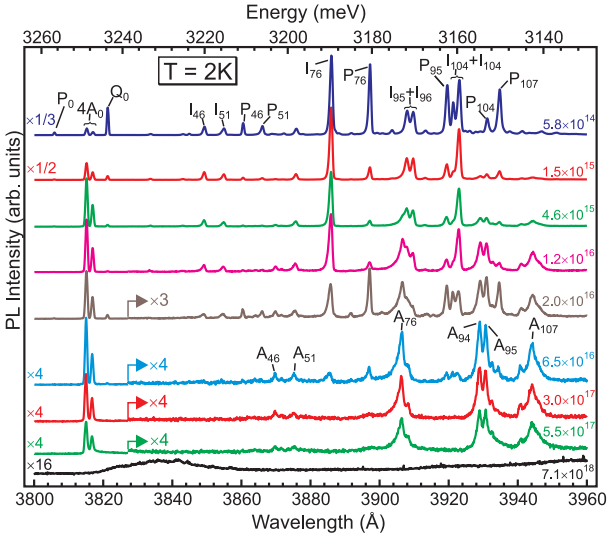

FIG. 1. PL spectra at 2 K of 4H-SiC free-standing uncompensated epilayers with different Al-doping concentrations, as denoted for each spectrum. Different scaling factors are applied to some of the spectra (shown to the left of the curves) in order to make them commensurate for display. The no-phonon lines of the Al-BE (the doublet $4A_0$) and N-BE (P_0, Q_0) are marked, as well as their phonon replicas, A_{xx} and P_{xx}, respectively, as explained in text. The phonon replicas of the free-exciton emission are also denoted in a similar manner as I_{xx}. Note also the additional scaling factors applied within four of the spectra in order to make visible the weak Al-BE replicas.

The PL spectra at 2 K of the free-standing samples labeled with the Al concentration are shown in Fig. 1. The spectra of the corresponding samples with substrate are essentially the same apart from some weak broad-band contribution originating from the substrate. The Al-related no-phonon lines (labeled by $4A_0$) and their phonon replicas (labeled by A_{xx})[25] are observed in all samples except for the sample with the highest Al concentration ([Al] = 7.1×10^{18} cm^{-3}). Here the subscript 'xx' denotes the approximate energy in meV of the phonon involved in momentum conservation. In the sample with the highest Al concentration ([Al] = 7.1×10^{18} cm^{-3}), a broad red-shifted band is observed instead of the sharp Al-related peaks, which is most likely associated with band gap narrowing and formation of an impurity band as a consequence of the overlapping wave functions of neighboring acceptors. On the other hand, the PL lines related to the N-BE are prominent only in the sample with the lowest [Al] = 5.8×10^{14} cm^{-3}. The N-BE zero-phonon lines P_0 and Q_0 corresponding to the N-BE excitons at hexagonal and cubic sites, respectively, as well as some of the prominent replicas of the P_0 line (denoted P_{xx} with the same meaning of the subscript 'xx' as for the Al-related replicas) are labeled in the uppermost spectrum of Fig. 1.[26] The phonon replicas of the free-exciton emission are denoted in the same manner as I_{xx}.

None of the samples shows any detectable donor-acceptor pair (DAP) related lines or bands at 2 K. This is a consequence of and may serve as indication for uncompensated material. In the context of this work, by uncompensated material we understand the SiC epilayers in which the amount of ionized acceptors and donors is negligible compared to the acceptor and donor concentrations, respectively. Such situation may arise in two different cases. One of them is the case of very low doping levels, when the average distance between donors and acceptors is much larger than the effective Bohr radius of donor electrons (~15 Å for the nitrogen donor at the hexagonal site, which is shallowest and thus has the largest Bohr radius). Due to very low overlap between donor and acceptor wave functions in this case a negligible amount of donors and acceptors are ionized at 2 K and most donors and acceptors can be considered as isolated from each other. The other case addresses the situation of asymmetric co-doping, i.e., when the concentration of one of the species (acceptors in our case) is much larger than that of the other (donors). This is the case with all investigated samples ($N_D/N_A < 0.01$) except for the lowest-doped sample where $N_D/N_A \approx 0.07$. In this latter sample [Al] = 5.8×10^{14} cm^{-3}, [N] = 4×10^{13} cm^{-3}, one calculates average distances of the order of 1000 Å between donors, acceptors, as well as between the donor and acceptor in a donor-acceptor pair. Thus, in this particular sample the donors and the acceptors can be considered as isolated from each other. If we attempt to estimate the N-doping concentration [N] in this sample from the PL spectrum using the algorithm of Ref. [16], we obtain [N]≈ 1.3×10^{14} cm^{-3}, i.e., a factor of three overestimation. This is due to the diminished intensity of the free-exciton emission because of the presence of acceptors with concentration more than an order of magnitude larger than that of donors. Thus, the ratio of the

BE/FE emissions increases leading to overestimated [N]. However, as will be seen later, the Al-doping concentration can be estimated quite accurately. This is understandable, because the presence of donors in concentration more than an order of magnitude lower than that of acceptors has only very minor impact on the population of free excitons.

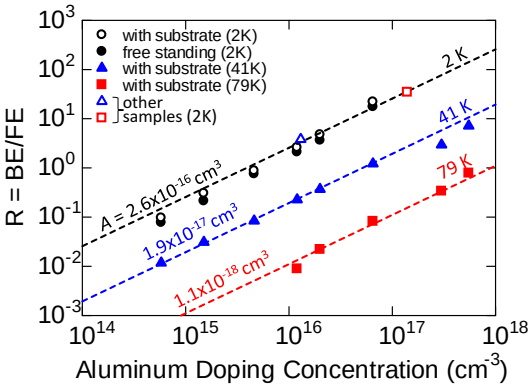

FIG. 2. The linear relationships between R and [Al] obtained from free-standing and as grown (with substrate) specimens from each sample at three different temperatures. Two other samples grown in different reactors are also included (open triangle and open square). The dotted lines represent the least-squares fit to the dependence of ln R vs. ln [Al] for each temperature. Note that in the logarithmic plot the three dotted lines are parallel with a slope equal to one, as expected for a linear dependence, $R = A\times[Al]$, i.e., one decade vertical corresponds to one decade horizontal change for each line. The slopes A for the three different temperatures were determined in accord with Eq. (1) to be 2.6×10^{-16}, 1.9×10^{-17}, and 1.1×10^{-18} cm^3 at 2, 41, and 79 K, respectively. In the logarithmic plot, these different values of A are associated with different vertical offsets of the least-squares line fits drawn in the figure.

For the determination of the integrated intensity ratio ($R = I_{BE}/I_{FE}$) we use line fitting of the two Al-related lines (denoted $4A_0$) and the strongest I_{76} phonon replica of the free exciton. We use least-squares fit using Gaussian and Maxwellian convoluted with Gaussian line shapes for the bound and free exciton lines, respectively, which provides accurate measures of the full width at half maximum (FWHM) and the amplitude of each peak. The latter Gaussian involved in the convoluted line shape is of fixed FWHM of 0.5 meV and mimics the spectrometer transfer function. The product of the amplitude with the FWHM is proportional to the integrated area beneath a peak, hence the I_{BE}/I_{FE} ratio is defined as $R = (A_1 + A_2)\Delta_{Al}/(A_{FE} \cdot \Delta_{FE})$, similar to the N-doping determination approach in Ref. [16]. Here A_1, A_2 and A_{FE} denote the amplitudes of the two Al-related lines and the free-exciton line, and Δ_{Al} and Δ_{FE} are the corresponding line widths (the linewidth Δ_{Al} is common for the two Al no-phonon lines). This definition is convenient because the amplitudes and peak widths can be estimated also manually from the spectra, thus eliminating the need for fitting. The dependence of R on [Al] at 2 K is displayed in Fig. 2 (black and white circles for the free-standing epilayers and epilayers with substrate, respectively). The relationship is clearly linear, $R = A\times[Al]$. The slope A is obtained from least-squares fit to the following equation,[17]

$$A = \exp\frac{1}{N}\sum_{i=1}^{N}(\ln R_i - \ln [Al]_i) \qquad (1)$$

where N is the number of experimental data points enumerated by the index i, and R_i and $[Al]_i$ are the values of R and [Al] for each sample. At 2 K the slope A is determined as $A = 2.6 \times 10^{-16}$ cm^3. The data at 2 K in Fig. 2 includes also two other uncompensated p-type epilayers grown in different reactors (open triangle and open square), which nicely confirm the same dependence. Thus, the data acquired at 2 K provide a confident and accurate evaluation of the Al concentration in uncompensated p-type 4H-SiC epilayers with [Al] $<\sim 2 \times 10^{17}$ cm^{-3}.

We have examined also other samples which, however, show quite strong N-BE emission suggesting significant compensation due to comparable N- and Al-doping concentrations (not shown). These compensated samples show lower R-ratio, as a consequence of the compensation. The main question arising in this context is whether the amplitude ratio of the Q_0 line and the stronger Al line can be used as a criterion justifying if the sample is compensated or not? The answer is positive, but it should be noted that the maximum Q_0/Al ratio for which a sample can be considered as uncompensated actually decreases with increasing [Al]. Thus, $Q_0/Al \approx 4$ for the sample with [Al] $= 5.8 \times 10^{14}$ cm^{-3} and compensation ratio 7%, but this sample fits well the linear dependence R([Al]). Three other samples, all showing $N_A - N_D$ in the low 10^{14} cm^{-3} display significantly underestimated [Al] as obtained from PL, but also $Q_0/Al \approx 20$ for all of them and thus the samples should be considered as compensated. This observation sets the lower bound for maximum Q_0/Al ratio for which the sample can be considered as uncompensated to around 4 when [Al] is in low-to-mid 10^{14} cm^{-3} range. However, the maximum Q_0/Al ratio for which the sample can be considered as uncompensated decreases with increasing [Al]. Thus, for instance, $Q_0/Al = 0.22$ for the sample with [Al] $= 1.5 \times 10^{15}$ cm^{-3} allows accurate [Al] determination using R, but a sample with similar concentration [Al] $= 2.8 \times 10^{15}$ cm^{-3} and larger $Q_0/Al = 0.62$ shows significant deviation below the R([Al]) dependence displayed in Fig. 2. The strongest N-BE lines, Q_0 and P_{76}, can be observed in all samples with [Al] $< 1\times10^{17}$ cm^{-3}. However, the Q_0/Al ratio for the rest of the samples obeying the linear dependence R([Al]) remains in the range 0.02–0.08. Thus, Q_0/Al of the order of few percent can be considered as a safe criterion for justifying uncompensated samples in the range [Al] $\sim$ mid 10^{15}–10^{17} cm^{-3}. At lower con-

centrations, samples with larger Q_0/Al ratio can be considered as uncompensated up to at least $Q_0/Al \sim 4$ at [Al] in the mid 10^{14} cm^{-3} range. The quoted figures for Q_0/Al should be considered only as a rough lower bound of the admissible Q_0/Al ratios allowing accurate determination of [Al] from the PL spectra provided, of course, that no other exciton-capturing impurities and defects in significant concentrations are present in the sample. Impurities, such as Ti, as well as defects, e.g., stacking faults, may capture significant amount of excitons and compete with the emission in the Al-related lines, but only traces of the D1 defect[27,28] and sometimes Ti-related luminescence[29] are observed in our samples, with intensity at least 2 orders of magnitude weaker than the $4A_0$ doublet.

The free-exciton emission (I_{76}) at 2 K becomes undetectable for samples with [Al] $> 2 \times 10^{17}$ cm^{-3}. In order to extend the range of [Al] which can be determined by PL towards higher concentrations, we conduct PL measurements at higher temperatures, as previously suggested for B-acceptors and P-donors in Si.[30] At higher temperatures a fraction of the Al-bound excitons are thermally dissociated from the acceptors and the free-exciton contribution to the spectrum increases. We have collected PL spectra from the same set of samples at ∼41 K and at ∼79 K. Fig. 3 shows the PL spectra of the sample with [Al] $= 5.5 \times 10^{17}$ cm^{-3} at various temperatures (2, 41, 79 K). The free-exciton emission (I_{76}) is not observed at 2 K, quite ambiguous at 41 K, but clearly detected at 79 K, which can be recognized by the asymmetric line shape of the free-exciton replicas as a consequence of the Maxwellian distribution of the free-exciton velocities in an indirect band-gap semiconductor.[31] On the other hand, the no-phonon emission from the Al-bound excitons ($4A_0$) is easily detected in this sample at all temperatures.

The relations between the ratio R and [Al] at 41 and 79 K for the p-type epilayers on substrate are also shown in Fig. 2 with filled triangles and squares, respectively. Due to line broadening and overlapping, however, we need to modify the algorithm of obtaining R at higher temperatures. At 41 and 79 K the free-exciton lines broaden significantly, so that several replicas in the vicinity of I_{76} merge into a single band with a sharp long-wavelength (low-energy) cutoff at ∼3886 Å. This band, denoted for convenience as I_{76} in Fig. 3, is separated from the strong replicas of the Al-lines (cf. Fig. 1), but it still contains contributions from the weaker Al_{46} and Al_{51} replicas clearly visible in the spectrum at 41 K in Fig. 3. At 79 K the free-exciton contribution to the spectrum increases while the Al-related contribution further decreases and becomes negligible in the I_{76} band. At both elevated temperatures we take as the free-exciton contribution in R the integrated intensity in the shaded area of this band (Fig. 3). The Al-related contribution at 79 K to the I_{76} band can be neglected even at the highest doping level investigated here, [Al] $= 5.5 \times 10^{17}$ cm^{-3}, for the following reasons. One estimates from the spectrum

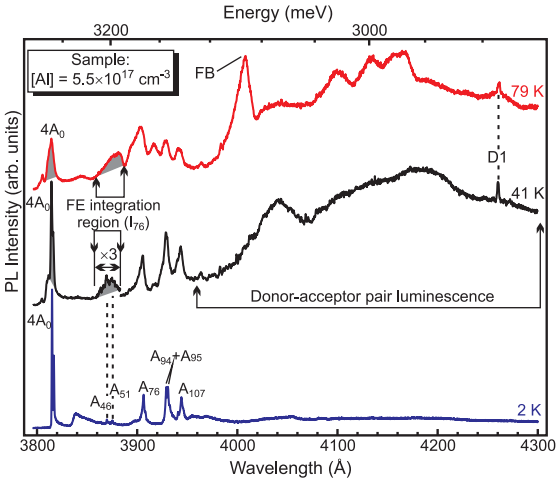

FIG. 3. Temperature dependence of the PL spectrum of the epilayer (on n-substrate) with doping concentration of 5.5×10^{17} cm^{-3}. The integrated intensities used for the definition of R are designated by the shaded areas in the spectra at 41 and 79 K. Note the scale change in the vicinity of I_{76} in the spectrum taken at 41 K manifesting the overlap of some Al-BE replicas with the free-exciton emission. The contribution of the Al-BE replicas in the vicinity of I_{76} is well visible at 41 K, but assumed negligible at 79 K, as discussed in text. The spectra at 41 K and 79 K illustrate also the appearance of donor-acceptor pair luminescence and the weak D1-defect center emission. 'FB' indicates the free-to-bound emission peak.

at 2 K in Fig. 3 that the integrated area beneath the Al_{46} and Al_{51} replicas is about $4 - 5\%$ of the area of the $4A_0$ peaks. Assuming similar intensity distribution between the replicas and $4A_0$ in the spectrum at 79 K one may conclude that the area of I_{76} may be overestimated due to the contribution of Al_{46} and Al_{51}, but only by $< 4\%$ because R = 0.78 at 79 K for this particular sample. Hence, we neglect the contribution of the Al-related replicas to the I_{76} band. Thus, the two points of high Al doping concentration ([Al] $> 1 \times 10^{17}$ cm^{-3}) deviate from the linear relationship at 41 K due to overlap of I_{76} with Al-replicas, but they are on the line for the same samples at 79 K. The Al-related no-phonon lines also broaden at higher temperatures, and new lines associated with excited states of the Al-bound exciton appear at higher energies. Similarly to the free exciton band, we take for the bound-exciton contribution in R the integrated intensity of the two strongest lines denoted $4A_0$ (merging in a band at 79 K, see the shaded areas in Fig. 3). We notice that at 79 K the Al-related no-phonon lines vanish for [Al] $< 1 \times 10^{16}$ cm^{-3} as a consequence of the thermal dissociation of Al-BEs. Therefore, low temperature PL measurement (2 to 41 K) should be used for [Al] determination in lightly or moderately doped p-type 4H-SiC ([Al] $< 5 \times 10^{16}$ cm^{-3}), while liquid-nitrogen temperature enables measurement of [Al] up to at least $\sim 6 \times 10^{17}$ cm^{-3}. The calculated slopes A at the three different temperatures are given in Fig. 2 and are associ-

ated with different vertical offsets of the fitting lines. The quoted values are valid if the range of integration for the Al-BE lines is between 3810-3820 Å (3813-3819 Å) at 79 K (41 K), respectively, while the corresponding regions for the FE integration are 3858-3888 Å (3856-3887 Å).

We notice the appearance at 79 K of the previously reported[32,33] free-to-bound (FB) transition, as well as bands associated with donor-acceptor pair luminescence (DAPL, see Fig. 3). The FB peak at ∼3093 meV (4008 Å) is observed for all samples with [Al] $> 1 \times 10^{17}$ cm^{-3} owing to temperature induced dissociation of free excitons into free holes and electrons. The free electrons can recombine with acceptor-bound holes, and their Maxwellian velocity distribution near the bottom of the conduction band is reflected in the asymmetric shape of the FB peak. The appearance of DAPL at elevated temperatures is due to recombination of donor-bound electrons with acceptor-bound holes which, however, involve excited states of the donor/acceptor. The excited states may overlap significantly since they have much larger orbits than the corresponding ground states, thus explaining why the DAPL structures become detectable only at elevated temperatures.

In conclusion, we have established Al-doping calibration based on the linear relationship R = A×[Al] between the Al concentration [Al] and the integrated-intensity ratio R of the Al-BE PL lines ($4A_0$) to that of the FE I_{76} line at three different temperatures. We have demonstrated that the range of Al concentrations determinable by PL can be extended towards higher doping levels to above 5×10^{17} cm^{-3} by raising the sample temperature to ∼80 K, whereas low Al-doping concentrations require PL measurements at < 40 K. Thus, the calibration is applicable for uncompensated p-type 4H-SiC in a wide concentration range (mid 10^{14} up to mid 10^{17} cm^{-3}). The local nature of the PL measurement (laser spot ∼100 μm) provides possibility for mapping, which provides a versatile non-destructive tool for estimating the Al-doping level and its homogeneity on wafer scale, in contrast to other methods, which usually provide average values on macroscopic areas of the sample.

This work was supported by the Swedish Research Council (VR).

[1] M. Bhatnagar and B. J. Baliga, IEEE Trans. Electron Devices **40**, 645 (1993).
[2] M. Ruff, H. Mitlehner, and R. Helbig, IEEE Trans. Electron Devices **41**, 1040 (1994).
[3] A. Itoh, T. Kimoto, and H. Matsunami, IEEE Electron Device Lett. **16**, 280 (1995).
[4] W. Götz, A. Schöner, G. Pensl, W. Suttrop, W. J. Choyke, R. Stein, and S. Leibenzeder, J. Appl. Phys. **73**, 3332 (1993).
[5] J. Pernot, S. Contreras, J. Camassel, J. L. Robert, W. Zawadzki, E. Neyret, L. Di Cioccio, U. Umr, and M. Cedex, Appl. Phys. Lett. **77**, 4359 (2000).
[6] G. Rutsch, R. P. Devaty, W. J. Choyke, D. W. Langer, and L. B. Rowland, J. Appl. Phys. **84**, 2062 (1998).
[7] A. Koizumi, J. Suda, and T. Kimoto, J. Appl. Phys. **106**, 13716 (2009).
[8] G. Pensl, F. Schmid, F. Ciobanu, M. Laube, S. A. Reshanov, N. Schulze, K. Semmeiroth, H. Nagasawa, A. Schöner, and G. Wagner, Mater. Sci. Forum Vols. **433-436**, 365 (2003).
[9] A. Parisini and R. Nipoti, J. Appl. Phys. **114**, 243703 (2013).
[10] S. Asada, T. Okuda, T. Kimoto, and J. Suda, Appl. Phys. Express **9**, 41301 (2016).
[11] S. Contreras, L. Konczewicz, R. Arvinte, H. Peyre, T. Chassagne, M. Zielinski, and S. Juillaguet, Phys. Status Solidi A **214**, 1600679 (2017).
[12] R. P. Devaty and W. J. Choyke, Phys. Stat. Sol. (a) **162**, 5 (1997).
[13] W. Choyke, R.P. Devaty, Optical Properties of SiC, in *Silicon Carbide: Recent Major Advances* (W.J. Choyke, H. Matsunami, G. Pensl, Springer-Verlag Berlin Heidelberg, 2004), 413.
[14] E. Janzén, A. Gali, A. Henry, I.G. Ivanov, B. Magnusson, N.T. Son, Defects in SiC, in *Defects in Microelectronic Materials and Devices* (D.M. Fleetwood, S.M. Pantelides, R.D. Schrimpf, CRC Press, Taylor & Francis Group Boca Raton, 2009), 615.
[15] L.L. Clemen, M. Yoganathan, W.J. Choyke, R.P. Devaty, H.S. Kong, J.A. Edmond, D.J. Larkin, J.A. Powell, and A.A. Burk, Jr., Inst. Phys. Conf. Ser. No. 137, 251 (1994).
[16] A. Henry, O. Kordina, C. Hallin, C. Hemmingsson, and E. Janzén, Appl. Phys. Lett. **65**, 2457 (1994).
[17] I. G. Ivanov, C. Hallin, A. Henry, O. Kordina, and E. Janzén, J. Appl. Phys. **80**, 3504 (1996).
[18] M. Tajima, Appl. Phys. Lett. **32**, 719 (1978).
[19] M. Allardt, V. Kolkovsky, K. Irmscher, and J. Weber, J. Appl. Phys. **112**, 103701 (2012).
[20] K. D. Glinchuk and A. V Prokhorovich, Semiconductors **36**, 519 (2002).
[21] K. Lauer, C. Möller, D. Schulze, T. Bartel, and F. Kirscht, Phys. Status Solidi-Rapid Res. Lett. **7**, 265 (2013).
[22] H. F. Pen, F. A. J. M. Dreissen, S. M. Olsthoorn, and L. J. Giling, Semicond. Sci. Technol. **7**, 1400 (1992).
[23] S. Juillaguet, M. Zielinski, C. Balloud, C. Sartel, C. Consejo, B. Boyer, V. Soulière, J. Camassel, and Y. Monteil, Mater. Sci. Forum Vols. **457-460**, 775 (2004).
[24] H. Peyre, J. Sun, J. Guelfucci, S. Juillaguet, J. Hassan, A. Henry, S. Contreras, P. Brosselard, and J. Camassel, Mater. Sci. Forum Vol. **711**, 164 (2012).
[25] L. L. Clemen, R. P. Devaty, M. F. MacMillan, M. Yoganathan, W. J. Choyke, D. J. Larkin, J. A. Powell, J. A. Edmond, and H. S. Kong, Appl. Phys. Lett. **62**, 2953 (1993).
[26] I. Ivanov, U. Lindefelt, A. Henry, O. Kordina, C. Hallin, M. Aroyo, T. Egilsson, and E. Janzén, Phys. Rev. B **58**, 13634 (1998).
[27] L. Patrick and W.J. Choyke, Phys. Rev. B **5**, 3253 (1971).
[28] T. Egilsson, J.P. Bergman, I.G. Ivanov, A. Henry, and E. Janzén, Phys. Rev. B **59**, 1956 (1999).
[29] L. Patrick and W.J. Choyke, Phys. Rev. B **10**, 5091 (1974).
[30] T. Iwai, M. Tajima, and A. Ogura, Phys. Status Solidi C **8**, 792 (2011).
[31] T. Kimoto and J. A. Cooper, *Fundamentals of Silicon Carbide Technology* (John Wiley & Sons Singapore Pte. Ltd. , 2014).
[32] I.G. Ivanov, B. Magnusson, and E. Janzén, Phys. Rev. B **67**, 165211 (2003).
[33] M. Ikeda, H. Matsunami, and T. Tanaka, Phys. Rev. B **22**, 2842 (1980).